Rhodium-Carbon Monoxide Surface Chemistry: The Involvement of Surface Hydroxyl Groups on Al_2O_3 and SiO_2 Supports

P. Basu, D. Panayotov,† and J. T. Yates, Jr.*

Contribution from the Surface Science Center, Department of Chemistry, University of Pittsburgh, Pittsburgh, Pennsylvania 15260. *Received July 27, 1987*

Abstract: Direct spectroscopic evidence has been obtained indicating that specific OH groups on Al_2O_3 and SiO_2 are consumed as CO interacts with supported Rh crystallites to produce atomically dispersed $Rh^I(CO)_2(a)$. The reaction $(1/x)Rh^0_x + OH(a) + 2CO(g) \rightarrow Rh^I(CO)_2(a) + (1/2)H_2(g)$ has been shown to involve isolated OH(a) groups rather than H-bonded associated OH(a) species. The process may also be reversed upon treatment of the chemisorbed CO layer with $H_2(g)$ at temperatures above ~200 K. With the H_2 treatment, $Rh^I(CO)_2(a)$ species are converted back to Rh^0_x species as judged by changes in the IR spectrum where terminal CO(a) species (on Rh^0_x sites) and isolated OH(a) groups are regenerated. Comparative kinetic studies of OH(a) and OD(a) species indicate that the rate controlling step in the production of $Rh^I(CO)_2(a)$ does not exhibit a measurable kinetic isotope effect.

I. Introduction

The chemisorption-induced structural modification of supported metal aggregates is of importance in the field of heterogeneous catalysis. The state of aggregation in these systems can be expected to affect catalytic selectivity and activity. It is now well recognized that supported metal aggregates in the presence of adsorbates may lose their structural integrity while undergoing a variety of fragmentation and agglomeration processes.[1,2] For example, in a most illuminating paper by Van't Blik et al.,[3] EXAFS studies of Rh/Al_2O_3 provided direct confirmation that adsorption of CO significantly perturbs the Rh-Rh coordination number of the supported Rh clusters, leading to the formation of atomically dispersed Rh^I sites. The presence of isolated Rh sites capable of adsorbing two CO molecules as a *gem*-dicarbonyl species was first postulated by Yang and Garland[4] and was supported by later IR studies of Yates et al.[5,6] The *gem*-dicarbonyl entity, $Rh^I(CO)_2$, gives rise to a characteristic doublet in the IR spectrum at 2107 and 2034 cm^{-1}.[4]

It is also believed that surface ligands such as hydroxyl groups on oxide supports can be involved in the structural rearrangement of the metal aggregates and in changes in the oxidation state of the metal. The work of Brenner et al.[7,8] involving the thermal decomposition of metal carbonyls on Al_2O_3 has suggested that the reduction of OH groups on the support may be responsible for the formation of oxidized metal centers (such as Rh^I). Smith et al.[9,10] also postulated that surface hydroxyl groups were effective in the degradation and subsequent oxidation of zerovalent Rh carbonyl clusters supported on Al_2O_3.

Similar ideas were recently developed by Solymosi,[11,12] where an increase in the reduction temperature under $H_2(g)$ of the catalyst resulted in a decrease in intensity of the $Rh^I(CO)_2$ IR features, possibly due to a depletion of surface OH groups by pretreatment at high temperatures.

In this work, we show that supported Rh metal aggregates (Rh^0_x) are dispersed following the adsorption of CO, in the presence of isolated OH(a) species, to form $Rh^I(CO)_2$. For the first time direct spectroscopic evidence is obtained that indicates the involvement of specific OH groups in the disruptive oxidation of Rh^0_x crystallites to produce $Rh^I(CO)_2$. The results also indicate that the process can be reversed by treatment of the $Rh^I(CO)_2$ with $H_2(g)$, resulting in an aggregation of the atomically dispersed Rh^I sites to form Rh^0_x. Simultaneously, the OH groups previously consumed are regenerated at the surface. A brief report of this work has been published previously.[13]

II. Experimental Section

Infrared spectra were measured with use of a purged Perkin-Elmer Model PE-783 infrared spectrophotometer coupled with a 3600 data acquisition system for data storage and manipulation. The stainless steel UHV sample cell used for the spectroscopic measurements has been described previously.[14] Basically, it consists of a main cell body containing a CaF_2 disk that serves as the sample holder, held in place by a Cu support ring. Using either cooled or heated $N_2(g)$, the sample temperature can be conveniently regulated. The cell body is contained within two CaF_2 optical windows sealed in standard stainless steel flanges, permitting IR measurements in the 4000–1000 cm^{-1} spectral range. The IR cell is attached to a grease-free all-metal gas handling system and is maintained typically at a base pressure $P \leq 1 \times 10^{-8}$ Torr by a 20 L/s ion pump. Rough pumping is achieved with a zeolite sorption pump. The sample preparation procedure essentially consists of slurrying known amounts of $Rh^{III}Cl_3(aq)$ and either Al_2O_3 or SiO_2 in a mixture of H_2O/acetone. The resultant slurry is sprayed onto one-half side of the hot (50 °C) CaF_2 disk (sample holder) such that the solvents are flash evaporated leaving a uniform powder deposit. The other half of the CaF_2 plate is sprayed with metal-free support material in an identical manner. When the cell is laterally translated in the IR beam path, this "half-plate" method allows us to observe and spectroscopically compensate for any chemistry occurring on the support itself which has been treated under identical conditions as the catalyst.

The CaF_2 disk is then mounted in the IR cell and the following pretreatment steps employed: (a) outgassing at 300 K; (b) catalyst decomposition at 473 K for ≥12 h; and (c) reduction at 473 K by several successive exposures of ~400 Torr of $H_2(g)$ for 15–240 min; after each exposure for a specific time period, the cell is evacuated for ~30 min. To achieve exchange of OH groups for OD, the catalyst was reduced in $D_2(g)$. The H_2 and D_2 were obtained from Matheson in a high-pressure cylinder with a purity of 99.995% and 99.95%, respectively. The CO used

† Permanent address: Institute of General and Inorganic Chemistry, Bulgarian Academy of Sciences, 1040 Sofia, Bulgaria.

* Author to whom correspondence should be addressed.

(1) Moskovits, M., Ed. *Metal Clusters*; John Wiley: New York, 1986.
(2) Gates, L. C.; Guczi, L.; Knözinger, Eds. *Metal Clusters in Catalysis*; Elsevier: New York, 1986.
(3) Van't Blik, H. F. J.; Van Zon, J. B. A. D.; Huizinga, T.; Vis, J. C.; Koningsberger, D. C.; Prins, R. *J. Am. Chem. Soc.* **1985**, *107*, 3139.
(4) Yang, A. C.; Garland, C. W. *J. Phys. Chem.* **1957**, *61*, 1504.
(5) Yates, J. T., Jr.; Duncan, T. M.; Vaughan, R. W. *J. Chem. Phys.* **1979**, *71* (*10*), 3908.
(6) Yates, J. T., Jr.; Duncan, T. M.; Worley, S. D.; Vaughan, R. W. *J. Chem. Phys.* **1979**, *70* (*03*), 1219.
(7) Brenner, A.; Hucul, D. A. *J. Catal.* **1980**, *61*, 216.
(8) Hucul, D. A.; Brenner, A. *J. Phys. Chem.* **1981**, *85*, 496.
(9) Smith, A. K.; Hugues, F.; Theolier, A.; Basset, J. M.; Ugo, R.; Zanderighi, G. M.; Bilhou, J. L.; Bilhou-Bougnal, V.; Graydon, W. F. *Inorg. Chem.* **1979**, *18* (*11*), 3104.
(10) Bilhou, J. L.; Bilhou-Bougnal, V.; Graydon, W. F.; Basset, J. M.; Smith, A. K.; Zanderighi, G. M.; Ugo, R. *J. Organomet. Chem.* **1978**, *153*, 73.
(11) Solymosi, F.; Pasztor, M. *J. Phys. Chem.* **1985**, *89*, 4789.
(12) Solymosi, F.; Pasztor, M. *J. Phys. Chem.* **1986**, *90*, 5312.
(13) Basu, P.; Panayotov, D.; Yates, J. T., Jr. *J. Phys. Chem.* **1987**, *91*, 3133.
(14) Beebe, T. P.; Gelin, P.; Yates, J. T., Jr. *Surf. Sci.* **1984**, *148*, 526.

0002-7863/88/1510-2074$01.50/0

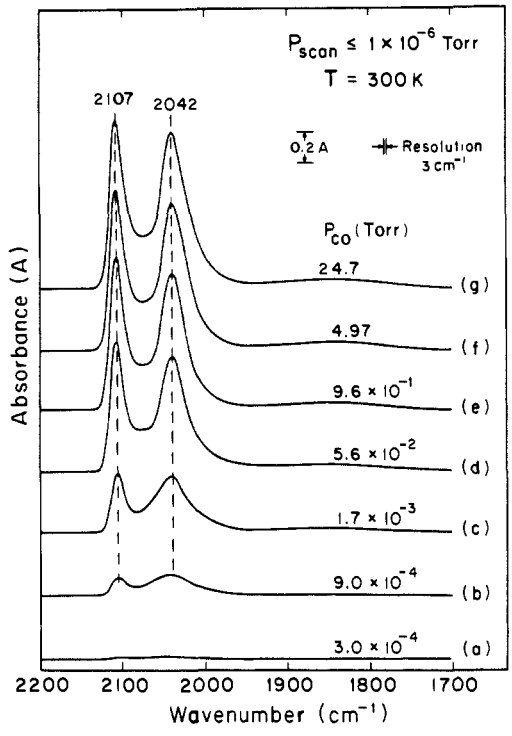

Figure 1. Infrared spectra for CO chemisorption on 2.2% Rh/Al_2O_3.

for adsorption studies had a purity level of 99.999% and was obtained from Scientific Gas Products in a break-seal glass storage bulb. The cell temperature was controlled between 90 and 300 K (to ±2 K) by adjusting the flow of the $N_2(l) + N_2(g)$ coolant through the Cu support ring. For the deuterium kinetic isotope effect (DKIE) experiments, the liquid-N_2 flow was completely shut off to warm the cell rapidly. Temperature and cell pressure during the spectral scan for each experiment are given in the respective figures.

The mass of Rh employed in these experiments ranges from 2.3–2.5 mg in separate samples for the 10 wt % loading, from 0.46–0.48 mg for the 2.2 wt % loading, and 0.06 mg for the 0.2% loading. A total sample weight of 22–27 mg was sprayed uniformly over a one-half plate (CaF_2 disk) area of 2.53 cm^2 yielding a final deposit surface density (Rh + Al_2O_3) of 8.7–10.7 × 10^{-3} g/cm^2 for the various samples. The Al_2O_3 used was Degussa Al_2O_3–C and the SiO_2 was Aerosil 200. For the DKIE experiments a loading of 2.2 wt % Rh/Al_2O_3 was employed.

The spectra presented were obtained with a slit program yielding a maximum resolution of 3.2 cm^{-1} with typical data acquisition times of 5 s/cm^{-1} for the ν_{OH} region and 0.85 s/cm^{-1} for the ν_{CO} region, acquired at 1 point/cm^{-1}. For the DKIE experiments the region between 2075 and 2125 cm^{-1} was scanned every 30 s. The data for the difference spectra were smoothed with a 19-point smoothing routine.

III. Results

A. Infrared Studies of CO Chemisorption on Rh/Al_2O_3 and Rh/SiO_2. IR spectra for the chemisorption of CO on 2.2% Rh/Al_2O_3 are shown in Figure 1. The *gem*-dicarbonyl species, $Rh^I(CO)_2$, is the predominant adspecies observed over the entire CO exposure range, in accordance with earlier experimental investigations[15] for the same level of Rh dispersion. The features at 2107 and 2042 cm^{-1} are attributed to the symmetric and asymmetric carbonyl stretching frequencies of $Rh^I(CO)_2$. No coverage dependent frequency shifts in the doublet features are observed confirming that $Rh^I(CO)_2$ exists as atomically dispersed Rh sites as proposed by Yates.[5,6]

Analogous spectra for CO adsorption on 10% Rh/SiO_2 are shown in Figure 4. The vibrational feature at 2048–2067 cm^{-1} is attributed to terminally bonded CO

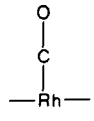

(15) Cavanagh, R. R.; Yates, J. T., Jr. *J. Chem. Phys.* **1981**, *74* (7), 4150.

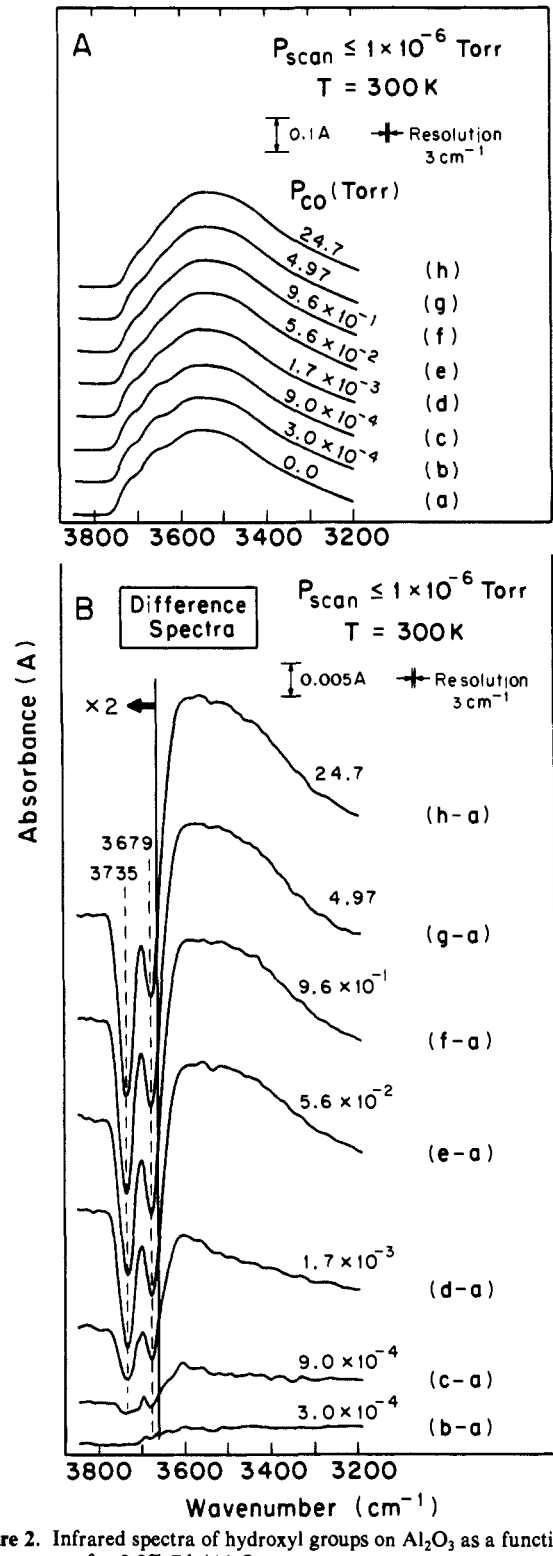

Figure 2. Infrared spectra of hydroxyl groups on Al_2O_3 as a function of CO exposure for 2.2% Rh/Al_2O_3.

while the broad spectral band between 1900 and 1925 cm^{-1} is due to the bridge-bonded CO[4].

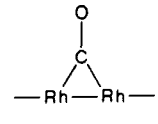

These two kinds of chemisorbed species are believed to form on metallic Rh sites in larger crystallites (Rh^0_x).[6] The terminal and bridge-bonded CO species are first to develop at low CO exposures, and the former remains the predominant spectral feature over the entire CO exposure range. For Rh/SiO_2 it was found that the

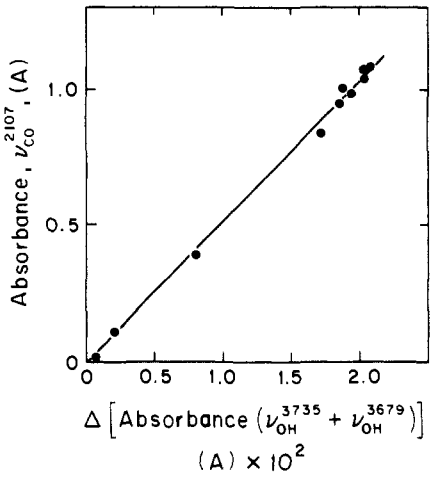

Figure 3. Correlation of $Rh^{I}(CO)_2$ formation with OH depletion for 2.2% Rh/Al_2O_3.

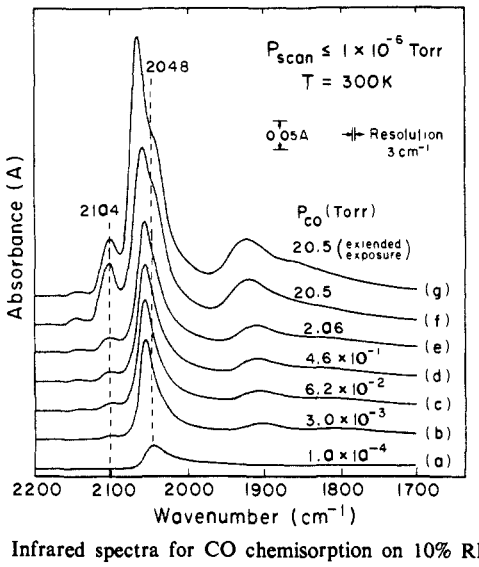

Figure 4. Infrared spectra for CO chemisorption on 10% Rh/SiO_2.

development of the doublet due to $Rh^{I}(CO)_2$ is relatively less intense as compared to the same Rh concentration in Rh/Al_2O_3 preparations (experiments not shown). This is in accordance with observations by others,[10,16] where $Rh^{I}(CO)_2$ on SiO_2 is formed to an appreciable extent only at relatively high Rh dispersion and at high temperature and CO pressure.

Simultaneous developments in the ν_{OH} region for Rh/Al_2O_3 and Rh/SiO_2 at various Rh loadings are shown in Figures 2, 5, and 6. In agreement with the model for surface hydroxyl groups on Al_2O_3 proposed by Peri,[17] the small shoulders at ~3732–3735 and 3679–3683 cm^{-1} on Al_2O_3 are assigned to isolated OH groups whereas the broad ν_{OH} feature, centered at ~3550 cm^{-1} for Al_2O_3, is believed to be caused by vibrations of H-bonded (associated) hydroxyl groups. For SiO_2 (Figure 5), the features due to the stretching vibrations of OH groups are less complex. The sharp band at 3743 cm^{-1} is universally assigned to an isolated surface OH group which is unperturbed by its neighbors. A tail in the 3700–3500-cm^{-1} region is due to weakly H-bonded groups, and the weak and unresolved absorption in the 3500–3400-cm^{-1} region is caused by strongly H-bonded OH groups or residual H_2O that is molecularly adsorbed.[18,19] Perturbations of specific OH groups are most easily seen in the difference spectra in Figures 2B, 5B,

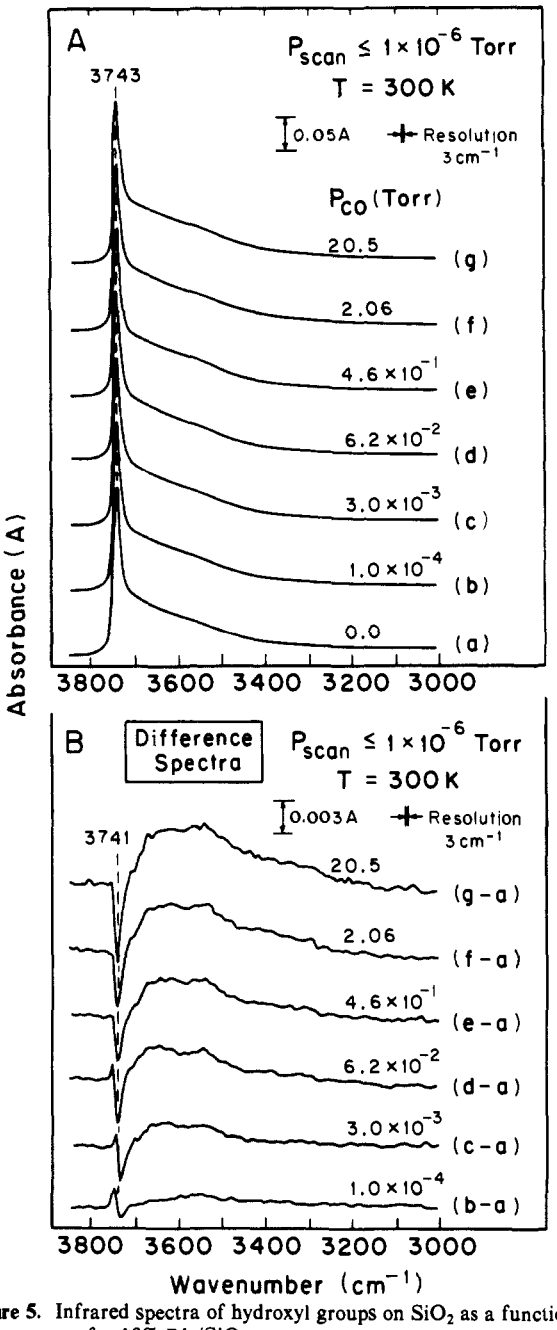

Figure 5. Infrared spectra of hydroxyl groups on SiO_2 as a function of CO exposure for 10% Rh/SiO_2.

and 6B for both Rh/Al_2O_3 and Rh/SiO_2 with increasing CO coverage. The difference spectra are calculated by subtracting the background (spectrum a in Figures 2A, 5A, and 6A) from each subsequent spectrum. The sequence of difference spectra are shown in Figures 2B, 5B, and 6B. Sharp negative features at 3731–3735 and 3675–3683 cm^{-1} for Rh/Al_2O_3 and a single negative feature at 3741 cm^{-1} for Rh/SiO_2 are observed to develop, *representing the depletion of specific isolated OH groups from the support surface as the $Rh^{I}(CO)_2$ species is produced.* The depletion of surface OH groups as a function of increasing CO exposure was not observed in control experiments on the metal-free support.

The relationship between the consumption of isolated OH groups and the population of $Rh^{I}(CO)_2$ for Rh/Al_2O_3 is shown in Figure 3. Here the total absorbance (difference) of the two negative ν_{OH} features is plotted as a function of the positive absorbance of the 2107-cm^{-1} vibrational feature due to $Rh^{I}(CO)_2$ formation. An excellent linear relationship is observed between the depletion of surface OH groups and the increase of $Rh^{I}(CO)_2$ coverage over the entire CO exposure range. Similar correlations are found for the higher loading of Rh/Al_2O_3 and for Rh/SiO_2.

(16) Worley, S. D.; Rice, C. A.; Mattson, G. A.; Curtis, C. W.; Guin, J. A.; Tarrer, A. R. *J. Phys. Chem.* **1982**, *86*, 2714.
(17) Peri, J. B.; Hannan, R. B. *J. Phys. Chem.* **1960**, *64*, 1526.
(18) Hair, M. L. *Infrared Spectroscopy in Surface Chemistry*; Marcel Dekker: New York, 1967; p 83.
(19) Peri, J. B. *J. Phys. Chem.* **1966**, *70* (9), 2937.

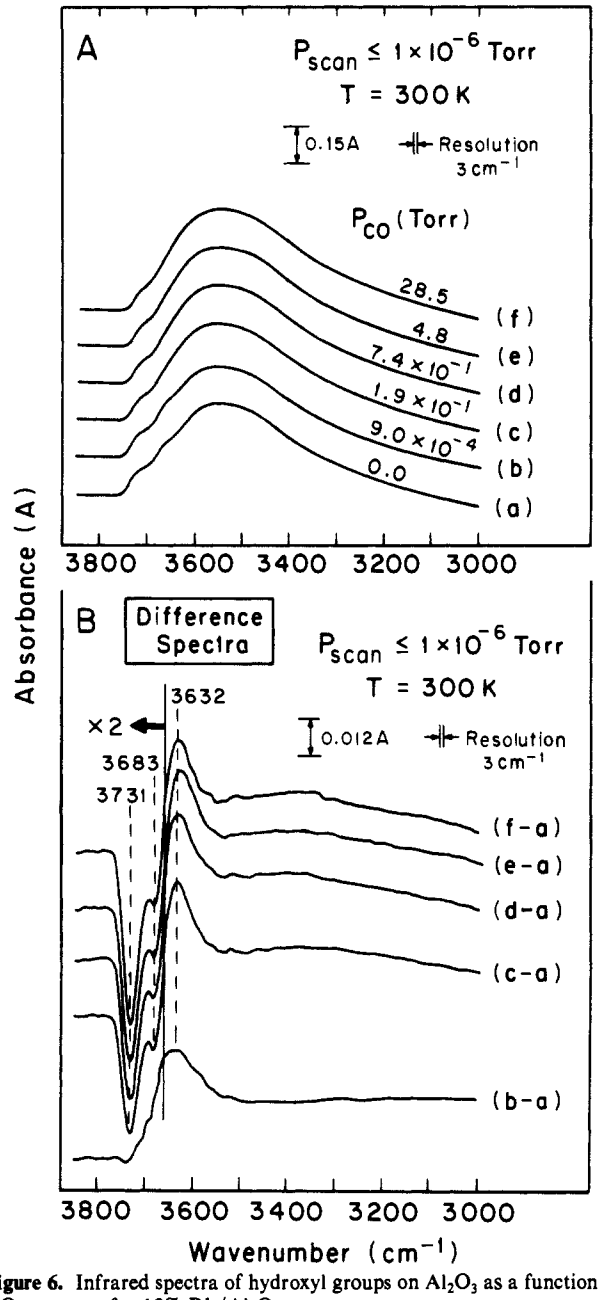

Figure 6. Infrared spectra of hydroxyl groups on Al_2O_3 as a function of CO exposure for 10% Rh/Al_2O_3.

As seen in Figures 2B, 5B and 6B, with increasing CO exposure a broad positive absorbance feature is also observed with frequency between 3450 and 3650 cm^{-1} for Rh/Al_2O_3 and at ~3610 cm^{-1} for Rh/SiO_2. This is the region in which vibrational frequencies due to associated OH groups are typically observed (as discussed previously). A closer look at the spectra (Figures 2A, 5A, and 6A) indicates that the presence of chemisorbed CO causes the following changes in the associated OH stretching region: (1) an increase in the total integrated absorbance of the feature, and (2) an increase in the full width at half maximum. These changes are characteristic of physisorption processes on OH groups typically via H bonding.[20-22] A linear correlation between the loss of OH intensity in the isolated OH species and the gain in integrated intensity in the associated OH species does not seem to exist here. Thus the positive absorbance difference seen in the associated ν_{OH} region is not related to a simple conversion of isolated OH groups to associated ones. This has further been verified by $H_2(g)$ treatment of the chemisorbed CO layer. With increasing exposure to $H_2(g)$ as $Rh^I(CO)_2$ species are destroyed, the specific isolated OH groups initially consumed during $Rh^I(CO)_2$ production are regenerated at the surface, while the positive absorbance feature in the associated ν_{OH} region still continues to increase in intensity (as discussed in the following section). Thus it is clear that spectral changes in the associated ν_{OH} region are not correlated with the production of $Rh^I(CO)_2$.

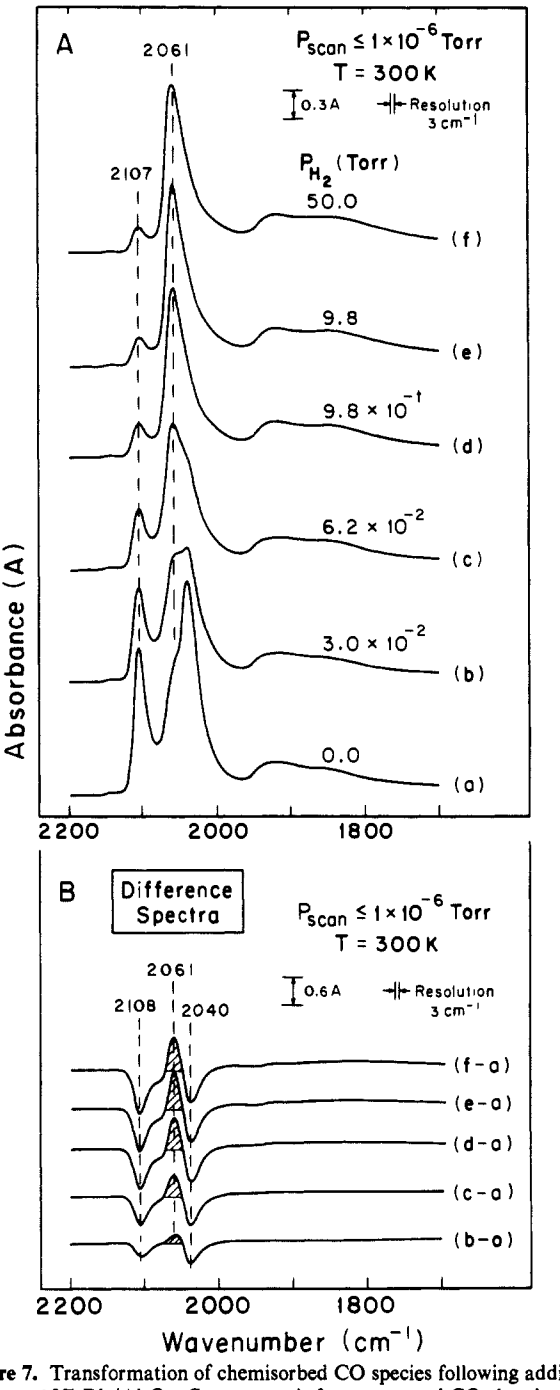

Figure 7. Transformation of chemisorbed CO species following addition of H_2 on 10% Rh/Al_2O_3. Spectrum a is for a saturated CO chemisorbed layer.

B. Interaction of $H_2(g)$ with Chemisorbed CO on Rh/Al_2O_3. Spectral changes that occur with increasing exposure of $H_2(g)$ to chemisorbed CO (on 10% Rh/Al_2O_3) are shown in Figure 7. It should first be pointed out that as compared to the chemisorbed CO layer on 2.2% Rh/Al_2O_3, the saturated CO layer on 10% Rh/Al_2O_3 (Figure 7, spectrum a) is characterized by a greater intensity contribution due to terminally bonded CO (2061 cm^{-1}) and bridge-bonded CO (1925–1875 cm^{-1}). This indicates that

(20) (a) Beebe, T. P.; Gelin, P.; Yates, J. T., Jr. *Surf. Sci.* **1984**, *148*, 526. (b) Beebe, T. P., Jr.; Yates, J. T., Jr. *Surf. Sci.* **1985**, *159*, 369.
(21) Pimentel, G. C.; McClellan, A. L. *The Hydrogen Bond*; W. H. Freeman and Co.: San Francisco, 1960.
(22) Crowell, J. E.; Beebe, T. P., Jr.; Yates, J. T., Jr., *J. Chem. Phys.* **1987**, *87* (6), 3668.

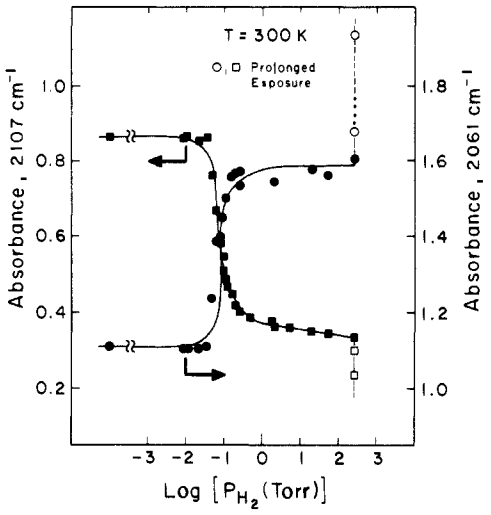

Figure 8. Correlation between depletion of $Rh^{I}(CO)_2$ and formation of $Rh^{0}_{x}(CO)$ on 10% Rh/Al_2O_3.

a larger fraction of Rh^{0}_{x} crystallite sites are present on the higher Rh concentration preparations of Rh/Al_2O_3. With increasing exposure to $H_2(g)$, the doublet feature due to $Rh^{I}(CO)_2$ decreases in absorbance while absorbance due to terminally bonded CO increases. This is seen clearly in Figure 7B where a sequence of difference spectra calculated by subtracting the background (spectrum a) from each subsequent spectrum is displayed. The increasingly negative absorbance difference at 2108 and 2040 cm^{-1} represents the depletion of $Rh^{I}(CO)_2$ while the systematic increase in intensity at 2061 cm^{-1} indicates an increase in population of CO bound terminally to Rh^{0}_{x} sites. Positive absorbance differences also occur in the bridged-CO region over a wide wavenumber range.

The depletion of $Rh^{I}(CO)_2$ can be directly correlated to the formation of $Rh^{0}_{x}(CO)$ as seen in Figure 8, where the absorbance of the 2107 cm^{-1} feature [$Rh^{I}(CO)_2$] and that of the 2061 cm^{-1} [$Rh^{0}_{x}(CO)$] is plotted as a function of the log H_2 partial pressure (P_{H_2}(Torr)). A systematic transformation of $Rh^{I}(CO)_2 \rightarrow Rh^{0}_{x}(CO)$ is seen to occur with increasing P_{H_2}. The transformation of the chemisorbed CO species is quite rapid within a narrow pressure range and occurs at pressures as low as 10^{-1} Torr. Furthermore, with prolonged exposures of $H_2(g)$ the depletion of $Rh^{I}(CO)_2$ and the concomitant formation of $Rh^{0}_{x}(CO)$ continues in much the same manner, confirming that the two processes are interrelated.

Spectral changes that occur in the ν_{OH} region with increasing H_2 exposure are shown in Figure 9. The following changes occur with H_2 exposure: (1) enhancement in the total integrated area both for the isolated (3722 cm^{-1}) and associated OH features, and (2) increase in the full width at half maximum of the IR feature due to associated OH groups.

The most striking observation is the development of the positive going ν_{OH} feature at 3722 cm^{-1} (Figure 9B); the absorption is within the IR spectral region attributed to isolated OH groups. This effect was also observed for Rh/SiO_2. Thus we find that with depletion of $Rh^{I}(CO)_2$, isolated OH groups are regenerated on the surface indicating that the process $Rh^{0}_{x}(+CO) \rightarrow Rh^{I}(CO)_2$, which involves surface OH groups, is reversible to a large extent. It should be noted that the resolution of vibrational features due to two distinct types of OH groups during the formation of $Rh^{I}(CO)_2$ has been lost and that the 3722-cm^{-1} feature is slightly broader and its frequency somewhat overlaps that of the original ν_{OH} features which disappeared upon $Rh^{I}(CO)_2$ formation. The positive absorbance change in the associated OH region cannot be correlated to the depletion of $Rh^{I}(CO)_2$ for the same reasons discussed previously; rather it is probably due to other side reactions that can be induced by $H_2(g)$.

The chemical and structural transformation induced by interaction of $H_2(g)$ with CO(a) is an activated process as seen in Figure 10. Here the temperature dependence of $Rh^{I}(CO)_2$ de-

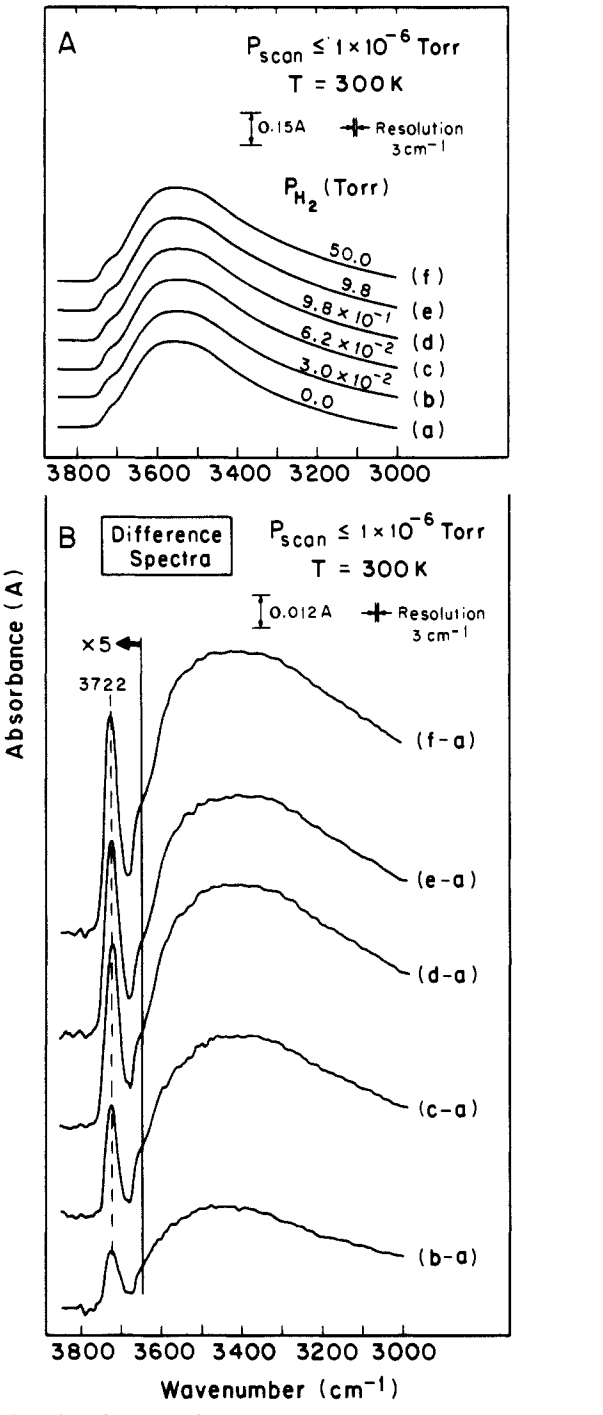

Figure 9. Infrared spectra of hydroxyl groups on Al_2O_3 during depletion of $Rh^{I}(CO)_2$ on 10% Rh/Al_2O_3.

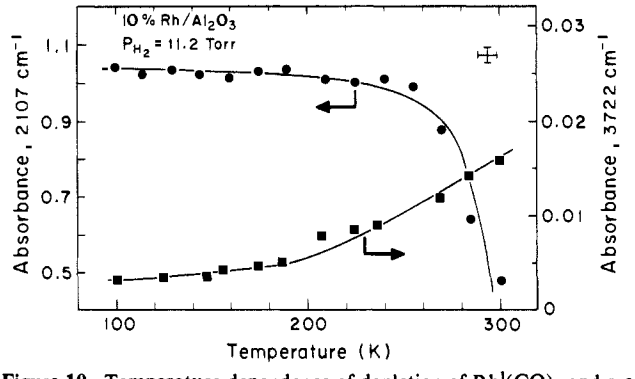

Figure 10. Temperature dependence of depletion of $Rh^{I}(CO)_2$ and restoration of surface hydroxyl group on Al_2O_3. The depletion of $Rh^{I}(CO)_2$ is induced by $H_2(g)$ treatment of CO chemisorbed on 10% Rh/Al_2O_3.

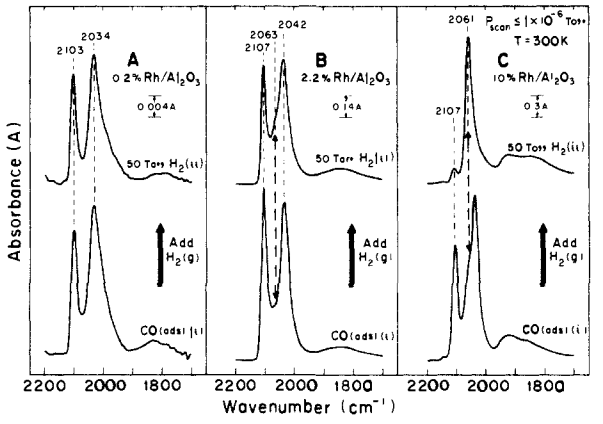

Figure 11. H_2-induced agglomeration of isolated Rh^I sites as a function of percent Rh/Al_2O_3. The bottom spectra are for a saturated CO chemisorbed layer. The top spectra are obtained following exposure of 50 Torr of H_2 (12 h) to the CO(a) layer.

pletion is correlated to the restoration of OH groups at the surface. Although the characteristic shape of each curve is somewhat different it is clearly seen that the H_2-induced reversibility of the reaction $Rh^0_x + 2CO \rightarrow Rh^I(CO)_2$ involving surface OH groups does have an activation barrier and the onset temperature for reaction is near ~200 K.

This process was also found to be dependent on the concentration of Rh atoms on the support. This is shown clearly in Figure 11. The three bottom spectra represent the characteristic IR spectrum for chemisorbed CO on the various dispersions of Rh/Al_2O_3. Note the wide range of the absorbance scale represented here. The relative ratio of terminally and bridge-bonded CO to $Rh^I(CO)_2$ increases with Rh loading, since a larger number of crystallite sites are present on the surface. Upon addition of H_2(g) (50 Torr, 12 hrs) no change is evident for the highest dispersion of Rh/Al_2O_3 (0.2%), whereas for 10% Rh/Al_2O_3 a dramatic difference is observed; the $Rh^I(CO)_2$ species are practically all depleted while the intensity due to $Rh_x(CO)$ is strongly enhanced (2061 cm^{-1}). Under the same conditions, for the 2.2% Rh/Al_2O_3 substrate, a small increase in intensity for linear bonded CO is beginning to be observed (shoulder at ~2063 cm^{-1}, Figure 11B). *It appears that the process $Rh^I(CO)_2$ $(+H_2) \rightarrow Rh^0_x(CO)$ is influenced by the proximity of the atomically dispersed sites (Rh^I) to Rh^0_x aggregates.*

C. Kinetic Studies of the Formation of $Rh^I(CO)_2$ on Al_2O_3(OH) and on Al_2O_3(OD). If the involvement of OH groups in the reaction $(1/x)Rh^0_x + yCO \rightarrow (y/2)Rh^I(CO)_2$ is considered to be rate determining, then a deuterium kinetic isotope effect would be expected in comparing OH and OD groups. Kinetic studies as a function of temperature were performed to search for a deuterium kinetic isotope effect. The temperature dependence of the rate of formation of $Rh^I(CO)_2$ on hydroxylated and deuteriated Al_2O_3 is shown in Figure 12, where the relative intensity of the 2108-cm^{-1} feature is plotted as a function of temperature. Each absorbance value was normalized to the maximum absorbance obtained at 300 K. A baseline absorbance, taken in preliminary experiments before exposure to CO, was first subtracted from each point. As indicated in the figure, the activated production of $Rh^I(CO)_2$ begins at precisely the same temperature in both cases (OH and OD) near 115 K. Furthermore the slope of both curves is identical up to 200 K. Small differences at higher temperatures are attributed to differences in CO(g) pressure for the two experiments and to increased experimental error in the high absorbance value range. We conclude from these results that the kinetics of Rh^I formation are not influenced by the isotopic composition of the surface hydroxyl groups.

IV. Discussion

A. Reactivity of Surface Hydroxyl Groups in the Formation of $Rh^I(CO)_2$. At the pretreatment temperature employed (473 K), the oxide support surface is covered to a large extent with hydroxyl groups. For Al_2O_3, Peri[23] and Knözinger[24] report that

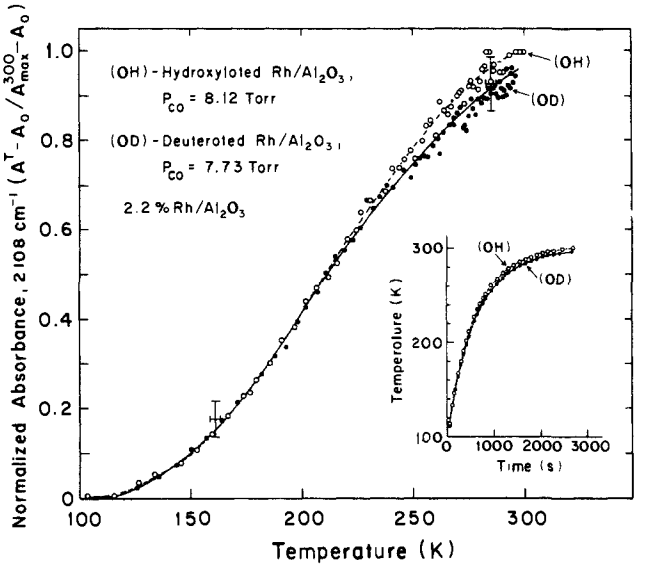

Figure 12. Temperature dependence of $Rh^I(CO)_2$ formation on hydroxylated (OH) and deuteriated (OD) Rh/Al_2O_3 (2.2%).

60–70% of the OH monolayer still persists at these temperatures, corresponding to ~8.9 OH/100 Å^2. For SiO_2 the value is 4.7 OH/100 Å^2.[25] On Al_2O_3-supported Rh, when $Rh^I(CO)_2$ species are formed, specific isolated OH groups are consumed (Figures 2 and 6). An increasing number of OH groups are depleted as the coverage of the $Rh^I(CO)_2$ increases for Rh/Al_2O_3. The intensity of the ν_{CO} 2107-cm^{-1} feature is linearly proportional to the total intensity difference of the negative-going ν_{OH} IR bands at 3735 and 3679 cm^{-1} (Figure 3) over the entire CO exposure range indicating a direct correlation between the consumption of these OH groups and the formation of $Rh^I(CO)_2$. This relationship was also observed for supports where a higher loading of Rh is present either on Al_2O_3 or SiO_2 (Figures 5 and 6). The consumption of surface OH groups as $Rh^I(CO)_2$ forms is most likely a general phenomenon for other oxide supports. Thus even when larger crystallites exist on the support their partial degradation to atomically dispersed Rh^I sites can be related to the depletion of specific isolated OH groups. The correlation between OH consumption and $Rh^I(CO)_2$ production has been verified by hydrogen treatment of the $Rh^I(CO)_2$ species on Al_2O_3. As $Rh^I(CO)_2$ is destroyed by H_2(g), the isolated OH groups that were consumed during $Rh^I(CO)_2$ production are regenerated. This reversible effect is discussed in a later section.

As seen in Figures 2, 5, and 6 only a small fraction of the total number of OH groups on Al_2O_3 and SiO_2 are involved in the formation of $Rh^I(CO)_2$. This is not surprising since ~10^{19} OH groups are present on the support surface in our samples as compared to only ~10^{18} Rh sites. The active hydroxyl groups for oxidation of Rh^0_x to Rh^I are the "isolated" OH groups giving the high-frequency ν_{OH} bonds that are sharp and easily discernible in our difference spectra for Rh/Al_2O_3 and Rh/SiO_2.

The specific activity of the isolated OH groups for the $Rh^0_x \rightarrow Rh^I$ conversion can be understood on the following basis: (a) The isolated OH groups are sterically more accessible as compared to those involved in H bonding with neighboring groups and can readily accommodate a large surface complex such as $Rh^I(CO)_2$. (b) The electron density around various kinds of OH groups may differ as suggested by Peri[26] and Knözinger,[24] making certain groups more conducive to reduction. Knözinger[24] has proposed a model where OH groups on Al_2O_3 exist in various geometrical configurations and as a result bear slightly different net charges. It follows that the surface OH groups would therefore differ in their reactivity toward oxidation of $Rh^0 \rightarrow Rh^I$.

(23) Peri, J. B. *J. Phys. Chem.* **1965**, *69* (*1*), 211.
(24) Kõnzinger, H.; Ratnasamy, P. *Catal. Rev.-Sci. Eng.* **1978**, *17* (*1*), 31.
(25) Kiseler, A. V.; Lygin, V. I. *Infrared Spectra of Surface Compounds*; John Wiley and Sons: New York, 1975; p 80.
(26) Peri, J. B. *J. Phys. Chem.* **1965**, *69*, 220.

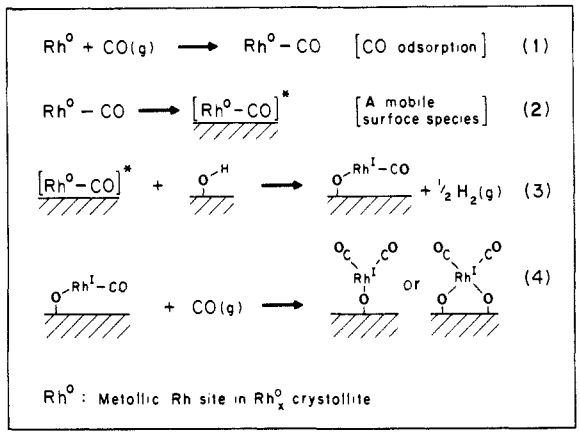

Figure 13. Postulated mechanism for the formation of $Rh^I(CO)_2$ on hydroxylated oxide supports. The stoichiometry of the $[Rh^0–CO]^*$ intermediate is unknown.

Thus, we postulate the mechanistic steps shown in Figure 13 that may occur upon treatment of Rh^0_x crystallites with CO(g) on hydroxylated oxide supports. Step 2 involves the weakening of Rh–Rh bonds by the adsorption of CO on Rh^0 surface sites. Such weakening in favorable sites leads to the liberation of a mobile $[Rh^0–CO]^*$ species that can migrate across the oxide surface to isolated OH groups (Step 3). The stoichiometry of the proposed mobile intermediate is unknown; it is possible that the fraction of the Rh crystallite that fragments and is mobilized consists of one or more Rh atoms and more than one CO ligand per Rh atom.

A number of research papers have suggested the involvement of OH groups in the structural and chemical transformation of supported-metal clusters.[1-3,7-12,27,28] Although our work does not yet offer an explanation of the exact mechanism by which surface OH groups are involved in the disruption and subsequent oxidation of Rh crystallites, we are in agreement with the mechanism proposed by Brenner et al.[7,8] In their scheme surface hydroxyl groups interact with zerovalent metal carbonyls $[M^0(CO)_x]$ during the decarbonylation process in a manner that leads to the oxidation of the metal atom (M^{n+}) with H_2(g) evolution:

$$M(CO)_x + n(\sigma\text{-OH}) \xrightarrow{\Delta} (\sigma\text{-O}^-)_nM^{n+} + (n/2)H_2 + xCO$$

B. Deuterium Kinetic Isotope Effect (DKIE). The deuterium kinetic isotope effect exists principally due to differences in the zero-point energy for the OH and OD groups. In establishing the DKIE an internal vibrational motion is selected to define the model reaction coordinate. The magnitude of the DKIE then depends upon the vibrational frequency of this molecular motion. It is clear from our measurements in Figure 12 that (1) we are dealing with an activated process leading to $Rh^I(CO)_2$[29] and (2) we are unable to detect a deuterium kinetic isotope effect through substitution of OD groups for OH groups on the Al_2O_3 support. There are several possible reasons for the lack of an observable isotope effect: (a) The rate-determining step in the proposed sequence of elementary steps 1–4 (Figure 13) may not involve H atom motions. (b) The rate-determining step may involve a low frequency H atom motion (such as the bending mode), giving a kinetic isotope effect that is too small for detection by our methods. (c) The overall kinetics of $Rh^I(CO)_2$ formation may be controlled by surface diffusional transport processes, as proposed previously by Yates and Kolasinski[30] for the reaction of Rh/Al_2O_3 + CO(g) leading to $Rh^I(CO)_2$.

C. Hydrogen-Induced Reversibility of the Process $(1/x)Rh^0_x + yCO \rightarrow (y/2)Rh^I(CO)_2$. An understanding of the interaction of chemisorbed CO with H_2(g) on supported Rh is of particular significance from the standpoint of various catalytic reactions. A number of papers in the literature have focused on this,[12,31-33] and recently Solymosi[12] has reviewed several possible reactions that might be expected to occur. In agreement with Solymosi's work,[12] we also observe that upon addition of H_2(g), $Rh^I(CO)_2$ is preferentially depleted while the coverage of terminally bound CO $[Rh^0_x(CO)]$ increases (Figure 7). Our work additionally demonstrates that as $Rh^I(CO)_2$ species are destroyed under H_2(g), isolated OH groups are regenerated on the support surface. Thus the reaction $(1/x)Rh^0_x + 2CO + (Al–OH) \rightarrow (Al–O)–Rh^I(CO)_2 + (1/2)H_2(g)$ can be reversed with the addition of H_2.

A possible mechanism that can be proposed for this interaction would involve the dissociation of $H_2(g) \rightarrow 2H(a)$ at metallic Rh sites. This is known to occur readily at 300 K from studies on Rh(111) single crystals.[34] Following the dissociative adsorption, H atoms can migrate across the support surface, a spillover effect spectroscopically observed by Cavanagh and Yates.[35] In this fashion, H encounters an anchored $Rh^I(CO)_2$ site. It is likely that the H atom donates its electron to Rh^I, reducing it to Rh^0, and then exists on the surface as a proton. The basic environment provided by the support would be expected to accept the proton and regenerate an OH group at the surface. This is consistent with the positive absorbance difference (Figure 9B) observed in the isolated OH stretching region, following addition of H_2(g) to CO(a). The $Rh^0(CO)_x$ species can then migrate across the surface, encounter Rh_x^0 nucleation sites, and expand its coordination number to reform larger metallic crystallites that are characterized by the strong ν_{CO} feature at 2061 cm^{-1}.

A number of papers[4,32,33,36-38] have proposed the existence of a rhodium carbonyl hydride

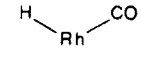

species as an intermediate in hydrogenation reactions. But the evidence for this has been somewhat inconclusive since the Rh–H stretching motions may overlap with the relatively intense ν_{CO} absorption bands in this IR spectral region. Although we cannot argue that the hydride species might exist under relatively high H_2 pressures and at a temperature >300 K, in our postulated mechanism above we do not propose the existence of the Rh(H)CO species. This is supported by the lack of a frequency shift or formation of new features in the ν_{CO} IR spectrum of 0.2% Rh/Al_2O_3 upon treatment with H_2(g) at 50 Torr (Figure 11A).

Thus the following summary can be made for the interaction of H_2(g) with $Rh^I(CO)_2$ species: (a) H_2 is not simply involved in a ligand exchange process where $Rh^I(CO)_2 \rightarrow Rh^I(H)CO$. (b) H_2 induces a structural rearrangement where atomically dispersed Rh^I sites are reduced and cluster to form larger metallic crystallites. This aggregation effect has been noted previously for treatment of oxide-supported metal carbonyl clusters.[9,10,27,28] (c) The CO chemisorbed as isolated $Rh^I(CO)_2$ species serves as a source of CO(a) on newly formed Rh^0_x sites; this is consistent with the enhancement of intensity of the $Rh^0_x(CO)$ terminal CO feature upon H_2 treatment. (d) Depletion of $Rh^I(CO)_2$ by H_2 treatment leads to regeneration of OH groups that give rise to IR intensity in the isolated ν_{OH} region.

One other effect that is evident from our results in Figures 7 and 8 is that even after prolonged exposure of H_2(g) a small amount of intensity due to $Rh^I(CO)_2$ is present. This is likely due to $Rh^I(CO)_2$ initially accommodated on special sites on the support surface. Differences in the basicity of the various types of surface sites are well recognized.[24,26] The slow depletion of these

(27) Thornton, E. W.; Knözinger, H.; Tesche, B.; Rafalko, J. J.; Gates, B. C. *J. Catal.* **1980**, *62*, 117.
(28) McNulty, G. S.; Cannon, K.; Schwartz, J. *Inorg. Chem.* **1986**, *25*, 2919.
(29) Wang, H. P.; Yates, J. T., Jr. *J. Catal.* **1984**, *89*, 79.
(30) Yates, J. T., Jr.; Kolasinski, K. *J. Chem. Phys.* **1983**, *79* (*2*), 1026.
(31) Fujimoto, K.; Kameyama, M.; Kunugi, T. *J. Catal.* **1980**, *61*, 7.
(32) Solymosi, F.; Tombācz, I.; Kocsis, M. *J. Catal.* **1982**, *75*, 78.
(33) Worley, S. D.; Mattson, G. A.; Caudill, R. *J. Phys. Chem.* **1983**, *87*, 1671.
(34) Yates, J. T., Jr.; Thiel, P. A.; Weinberg, W. H. *Surf. Sci.* **1979**, *84*, 427.
(35) Cavanagh, R. R.; Yates, J. T., Jr. *J. Catal.* **1981**, *68*, 22.
(36) Solymosi, F.; Erdōhelyi, A.; Kocsis, M. *J. Catal.* **1980**, *65*, 428.
(37) Henderson, M. A.; Worley, S. D. *J. Phys. Chem.* **1985**, *89*, 1417.
(38) McKee, M. L.; Dai, C. H.; Worley, S. D., submitted to *J. Phys. Chem.*

particular $Rh^I(CO)_2$ species may reflect the differences in reducing/oxidizing properties of these specific surface sites.

D. Agglomeration of Atomically Dispersed Rh^I. As discussed above the reduction of $Rh^I \rightarrow Rh^0$ and the subsequent aggregation in the presence of $H_2(g)$ occurs readily at $T \sim 200$ K and P_{H_2} as low as 10^{-1} Torr. The agglomerization is also kinetically controlled by the relative ratio of atomically dispersed (Rh^I) to crystallite (metallic Rh^0) sites as seen in Figure 11. This can be understood on the basis of our postulated mechanism above; the metallic Rh^0_x sites act as "feeder sites" for hydrogen atoms that induce the reductive agglomerization. With a higher loading of Rh/Al_2O_3 (10% Rh/Al_2O_3) these "feeder sites" are in close proximity to the isolated Rh^I sites. As a result the availability of migrating H atoms is considerably enhanced. On the other hand when almost no metallic Rh^0_x sites are present (0.2% Rh/Al_2O_3) this process is inhibited (Figure 11A).

V. Summary and Conclusions

On the basis of the results of this work, the following conclusions can be made: (1) A general phenomenon, common for OH groups on both Al_2O_3 and SiO_2, has been observed in which the reaction $(1/x)Rh^0_x + OH + 2CO(g) \rightarrow Rh^I(CO)_2 + (1/2)H_2(g)$ occurs. This reaction leads to a significant structural degradation of oxide-supported Rh catalysts. (2) The oxidation process above can be reversed by $H_2(g)$ addition to $Rh^I(CO)_2$ on either Al_2O_3 or SiO_2 supports. (3) The oxidation process in (1) above does not exhibit a deuterium kinetic isotope effect. (4) The H_2-induced reduction of $Rh^I(CO)_2$ to Rh^0_x depends upon the presence of Rh^0_x sites to provide H(ads) species in a spillover mechanism. (5) Direct spectroscopic evidence for the specific involvement of isolated surface OH groups in the oxidation of Rh^0_x sites to Rh^I sites has been obtained.

Acknowledgment. We acknowledge, with thanks, the support of this work by the Office of Basic Energy Sciences, DOE. One of us (P.B.) is grateful for a supported educational leave from Alcoa. Another (D.P.) acknowledges with thanks the support of the NSF Eastern European Program, Grant. No. INT-8513805.

Registry No. Rh, 7440-16-6; CO, 630-08-0.

Methoxyethylene Ozonide: Analysis of the Structure and Anomeric Effect by Microwave Spectroscopy and ab Initio Techniques[1]

Marabeth S. LaBarge,[‡] Helmut Keul,[†,‡] Robert L. Kuczkowski,*[‡] Markus Wallasch,[§] and Dieter Cremer*[§]

Contribution from the Department of Chemistry, The University of Michigan, Ann Arbor, Michigan 48109, and Lehrstuhl für Theoretische Chemie, Universität Köln, D-5000 Köln 41, Federal Republic of Germany. *Received July 8, 1987*

Abstract: Fifteen isotopic species of methoxyethylene ozonide (3-methoxy-1,2,4-trioxolane) were synthesized and their microwave spectra assigned. The dipole moment was determined as 1.99 (4) D. The structure was determined from the rotational constants by both least-squares (r_o) and Kraitchman substitution (r_s) methods. Methoxyethylene ozonide has a peroxy envelope ring conformation and an axial methoxy substituent with a short C–OCH_3 bond. The methoxy group exhibits an unusual orientation anti to the ring hydrogen placing it over the ozonide ring. Ab initio calculations were performed to provide additional insights on the structural features. Both experimental and theoretical results are in accord with the anomeric and exo-anomeric effects.

The anomeric effect is a stereoelectronic phenomenon[2,3] which influences molecular conformations[4,5] and reactivities[6-11] of a wide range of species. This effect refers to the preference of an electronegative substituent to adopt an axial rather than the sterically favored equatorial orientation in heterocyclic rings.[3] A related stereoelectronic effect is the exo-anomeric effect. It is defined as the preference of R in OR (alkoxy) substituents for a gauche orientation relative to the ring heteroatom (X) in R–X–C–OR moieties. The anomeric and exo-anomeric effects have the same electronic origin associated with two-electron interactions between antibonding orbitals and filled bonding or nonbonding orbitals.

Concomitant with these conformational tendencies are significant changes in bond lengths from "normal" based on simple inductive effects by electronegative substituents. Numerous X-ray crystallographic investigations of carbohydrates have revealed a lengthening of the exocyclic C–X bonds when X is halogen and shortening when X is oxygen. Jeffrey and Pople[12] and others[13-15] have used ab initio molecular orbital techniques to study carbohydrate related moieties in order to correlate theoretical and experimental structural data.

A number of experimental and theoretical studies of fluoro-ozonides and other substituted ozonides have also provided data

[†] Present address: Lehrstuhl für Textilchemie und Makromoleculare Chemie, der RWTH, Aachen, Federal Republic of Germany.
[‡] The University of Michigan.
[§] Universität Köln.

(1) Presented in part as paper TA5, 41st Symposium on Molecular Spectroscopy, The Ohio State University, Columbus, OH, 1986.
(2) For recent reviews, see: (a) *Anomeric Effect: Origin and Consequences*; Szarek, W. A., Horton, D., Eds.; American Chemical Society: Washington, DC, 1979; ACS Symp. Ser. No. 87. Kirby, A. J. *Anomeric Effect and Related Stereoelectronic Effects at Oxygen*; Springer-Verlag: Berlin, 1983. (c) Deslongchamps, P. *Stereoelectronic Effects in Organic Chemistry*; Pergamon Press: London, 1983.
(3) Lemieux, R. U.; Chu, N. J. *Abstracts of Papers*, 133rd National Meeting of the American Chemical Society, San Francisco, CA; American Chemical Society: Washington, DC, 1958; No. 31N.
(4) Eliel, E. L. *Angew. Chem., Int. Ed. Engl.* **1972**, *11*, 739.
(5) de Hoog, A. J.; Buys, H. R.; Altona, C.; Havinga, E. *Tetrahedron* **1969**, *25*, 3365.
(6) Malatesta, V.; Ingold, K. U. *J. Am. Chem. Soc.* **1981**, *103*, 609.
(7) Beckwith, A. L. J.; Easton, C. J. *J. Am. Chem. Soc.* **1981**, *103*, 615.
(8) Bailey, W. F.; Croteau, A. A. *Tetrahedron Lett.* **1981**, *22*, 545.
(9) McKelvey, R. D.; Iwamura, H. *J. Org. Chem.* **1985**, *50*, 402.
(10) Danishefsky, S.; Langer, M. E. *J. Org. Chem.* **1985**, *50*, 3672.
(11) Deslongchamps, P. *Tetrahedron* **1975**, *31*, 2463.
(12) (a) Jeffrey, G. A.; Pople, J. A.; Radom, L. *Carbohydr. Res.* **1972**, *25*, 117. (b) Jeffrey, G. A.; Pople, J. A.; Radom, L. *Ibid.* **1974**, *38*, 81. (c) Jeffrey, G. A.; Pople, J. A.; Binkley, J. S.; Vishveshwara, S. *J. Am. Chem. Soc.* **1978**, *100*, 373. (d) Jeffrey, G. A.; Yates, J. H. *J. Am. Chem. Soc.* **1979**, *101*, 820.
(13) Wolfe, S.; Whangbo, M.-H.; Mitchell, D. J. *Carbohydr. Res.* **1979**, *69*, 1.

0002-7863/88/1510-2081$01.50/0